N73-16655

NASA TECHNICAL MEMORANDUM

NASA TM X-68182

NASA TM X-68182

CASE FILE COPY

THE EFFECT OF NOZZLE INLET SHAPE, LIP THICKNESS, AND EXIT SHAPE AND SIZE ON SUBSONIC JET NOISE

by W. A. Olsen, O. A. Gutierrez, and R. G. Dorsch
Lewis Research Center
Cleveland, Ohio

COPY

TECHNICAL PAPER proposed for presentation at
Eleventh Aerospace Sciences Meeting sponsored by the
American Institute of Aeronautics and Astronautics
Washington, D.C., January 10-12, 1973.

THE EFFECT OF NOZZLE INLET SHAPE, LIP THICKNESS, AND EXIT SHAPE AND SIZE ON SUBSONIC JET NOISE

by W. A. Olsen, O. A. Gutierrez, and R. G. Dorsch
Lewis Research Center

ABSTRACT

Far field noise data were taken for convergent nozzles of various shapes and sizes at subsonic velocities exceeding 400 feet per second. For a circular nozzle, the nozzle inlet shape and lip thickness had no effect on the noise level, directivity, or spectra when compared at the same nozzle exit diameter and peak exhaust velocity. A sharp edged orifice was one exception to this statement. Coannular nozzles can produce additional high frequency noise. Blunt ended centerbodies, where there is significant base drag, also generate significant additional noise.

The total noise power generation was essentially the same for circular, slot, and plug nozzles of good aerodynamic shape. The noise radiation patterns were essentially the same for these nozzle shapes except near the nozzle exhaust axis. These patterns were well described by $(1 - M_c \cos \theta_J)^{-3}$, except near the nozzle exhaust axis.

E-7289

INTRODUCTION

Aircraft jet noise is a major annoyance to the communities near airports. Subsonic jet noise generated by nozzles has been extensively measured by a number of recent investigators (refs. 1 to 4). Most of the data are for circular nozzles at ambient temperature. The effect on noise generation caused by different shaped circular nozzle inlets and nozzle lip thickness and length has not been adequately investigated (ref. 5). The effect on noise produced by changes in plug and slot nozzle geometry requires more work. More complete data for circular, plug, and slot nozzles would be helpful in evaluating the various jet noise theories.

A series of jet noise experiments were consequently performed at the NASA Lewis Research Center. The main purpose of these experiments was to determine the effect of physical variations in the shape of the common type of nozzles upon the noise generated. The secondary purpose was to obtain extensive noise data for circular, plug, and slot nozzles in order to evaluate jet noise theories.

The inlet shape of a 1.63 inch diameter circular nozzle was varied from a gradual area contraction to that of a sharp edged orifice. Lip thickness was varied, with the same gradual inlet, from very thin to very thick; and the effect of lip axial length (up to 30 diameters) on noise was investigated. The other nozzle exit plane shapes tested included

plug and slot nozzles, a coannular nozzle and some multijet nozzles. The plug nozzle annulus height and plug shape were varied. Slot nozzles of varying aspect ratio were tested. The data were essentially limited to subsonic velocities greater than 400 feet per second.

A small sample of the far field noise data taken in this program are presented herein as plots. These plots consist of noise radiation patterns, and sound pressure level and sound power level spectra. The data are compared to data taken by other investigators; and the results from two analytical models for jet noise are compared with these data.

APPARATUS AND PROCEDURE

Flow System and Valve Noise Quieting

Three similar rigs, of varying size, were used to obtain the jet noise data in this paper. Each flow system was attached to the NASA-Lewis laboratory air supply. Each system conceptually looked like the small rig shown on figure 1. The small rig consisted of the following (proceeding downstream): a 4-inch flow control valve; a valve noise quieting section; a long straight run of 4 inch pipe; and finally the test nozzle. The first valve noise quieting element was a perforated plate. Downstream of that was a large volume muffler with no line of sight. The muffler for the small rig is the four-chamber acoustically lined muffler shown on figure 1. The rigs used for the larger nozzle data (i.e., 4-in. nozzles and larger), used larger but similar flow hardware (see refs. 6 and 7). None of the nozzle jet noise data reported herein were affected by internal valve noise, either through the nozzle exit or by direct radiation through the fiberglass and lead vinyl insulation that was wrapped around the pipe. When the noise level was low, a small correction was made to the data below 400 Hz to account for background noise. Depending on the season, the nozzle stagnation temperature varied from 35° to 80° F.

Acoustic Instrumentation and Data Analysis

The noise data were measured outdoors with three types of semicircular microphone arrays that were centered on the nozzle exit (see fig. 1). Half-inch condenser microphones with windscreens were used with each. All arrays had a microphone radius of about 50 nozzle diameters to assure that the data were adequately in the far field. Most of the data were taken with a vertical semicircular microphone array, with open cell acoustic foam on the ground (fig. 1). This vertical array arrangement (with the foam) resulted in free field noise data for frequencies above 400 Hz. A horizontal semicircular array over hard ground (see fig. 1), was used for some of the data where only comparisons were to be made. The effect of ground reflections on this type of data was small and repeatable; therefore only an overall approximate correction to free field of the noise level was made. The 13-inch diameter nozzle data were taken with micro-

phones placed upon the ground at a 50-foot radius. These data were easily corrected to free field because they are 6 dB high at all frequencies of interest. Background noise had an effect upon the data below 400 Hz, whenever the noise level was low. Background noise was subtracted from the measured noise when it was at least 2 dB lower.

Most of the small nozzle data were measured using a vertical array of 9 or 10 microphones located on a semi-circle of radius 10 feet. The 4-inch nozzle data were measured by 11 microphones on a vertical semi-circle of 15 foot radius. The microphones were more closely spaced (10^{o} to 15^{o} intervals) near the nozzle jet than in the upstream quadrant (20^{o} to 30^{o} intervals). In the horizontal array, microphones were located in a horizontal plane that passed through the nozzle center line (fig. 1). The nozzle centerline was 4 feet above a smooth, flat, asphalt surface. The microphones were placed on a 10-foot radius circle, that was centered on the nozzle exit. In all arrays, the angle $\theta_I = 0^{o}$ is at the nozzle inlet.

Occasionally the wind would deflect the jet exhaust so that it would strike a microphone (with windscreen), which caused low frequency "wind" noise. To eliminate this error from the data, the low frequency part of the SPL spectrum from that microphone was rejected.

Noise data were taken at each microphone location for each run condition. The noise data were analyzed directly by an automated one-third octave band spectrum analyzer. The analyzer determined sound pressure level spectra, SPL, referenced to 0.0002 microbar (2×10^{-5} N/m^2). The resulting SPL spectra were then corrected for the small atmospheric attenuation (less than 1 dB) so that the reported data are lossless. They were then corrected for background noise and deflected jet "wind noise." These corrected SPL spectra were then used to compute the overall sound pressure level, OASPL, of each microphone position. Occasionally the peak SPL occurred too close to the highest frequency recorded (20 kHz), causing the computed OASPL to be too low. These SPL spectra were extrapolated and the OASPL was thereby corrected (less than 2 dB). The sound power level spectrum, PWL, and total sound power level, PWL_T, were computed by a spatial integration of these SPL spectra. The spatial integration used the "bread slice" elements for axisymmetric noise, as described in reference 8. Except for the slot nozzles, all the noise data reported in this paper are axisymmetric.

The condenser microphones were calibrated before and after each day of testing with a standard piston calibrator (a 124 dB tone at 250 Hz). The third-octave band analyzer was periodically calibrated and checked with a pink noise generator. Considering the microphone calibrations, periodic checks of the data system, and redundant data, it is estimated that the data are repeatable from day to day to within 1-1/2 dB. Much of the directly compared data were taken on the same day, so that these data were repeatable to about 1/2 dB.

Test Nozzles

Figure 2 contains sketches of the nozzle shapes tested. Table I contains the nozzle dimensions. The nozzle flange was far upstream, and the nozzle inlets were not so large that there would be a significant effect on the upstream quadrant of the noise radiation pattern. Figure 2(a) shows a series of short lip nozzles, of the same internal exit diameter, that have vastly different inlet and exit shapes. The two nozzles on the extreme left describe the standard shape circular nozzle used for many comparisons in this report. They have a gradual inlet and a thin short lip; and the flow coefficient is close to unity. The nozzles described on figure 2(b) have the same exit diameter and inlet shape, but differ in the lip length. Figure 2(c) contains a sketch of the shape of the slot nozzles tested. In one comparison the aspect ratio was varied through a variation in width, w, at a fixed slot height, h. Plug nozzles of the same exit area, with various annulus heights, h, and also various plug end shapes, were tested (figs. 2(d) and (e)). The effect of flow ventilation on multitube nozzle noise was partially studied by filling the space between the 19 tubes of the nozzle shown in figure 2(f) with modeling clay. Various shaped orifice holes of the same total exit area were cut in large flat plates as shown by figure 2(g). Figure 2(h) shows the coannular nozzle that was tested. With the exception of the long lip nozzles (figs. 2(b) and (f)), all nozzles had uniform velocity profiles across the nozzle exit.

Test Procedure

Far field noise and flow data were taken for a number of nozzle configurations at nozzle exhaust velocities, ranging from about 400 to 1100 feet per second. The nozzle configurations are shown on figure 2 and listed in table I. The data for nearly all the comparisons listed on a given figure were taken on the same day to take advantage of the high repeatability of such data.

RESULTS AND DISCUSSION

The results are discussed in three major sections. The first section considers free field noise data for standard shaped circular nozzles. These results are then compared to the results from two theoretical models. The second section considers variations of that standard circular shape, such as inlet shape, lip thickness, and length. The third section deals with noise from some nozzles of noncircular shape.

Noise from a Standard Shaped Circular Nozzle

A standard shaped circular nozzle is described by figures 2(a-1) and 2(a-2). It has an inlet with a gradual transition to the exit, the lip

is thin and short, and the flow coefficient is high with a uniform velocity profile at the exit. In this section, sound pressure level spectra, SPL, at $\theta_I = 90^o$ and also at other angles are given for a number of exhaust velocities. The sound power level spectra, PWL, are also plotted for a number of velocities and nozzle sizes. Noise radiation patterns, involving the overall sound pressure level, OASPL, and a correlation of the total sound power level, PWL_T, are also presented and compared to data from other experimentors. The SPL and OASPL are referenced to 0.0002 microbar, while the PWL and PWL_T are referenced to 10^{-13} watts.

Spectra. - Figure 3(a) gives the one-third octave free field sound pressure level spectra, SPL, at $\theta_I = 90^o$. The data are for a 4-inch diameter circular nozzle of standard shape at five subsonic velocities. The data are lossless, which means they were corrected for atmospheric attenuation. A comparison at $\theta_I = 90^o$ is useful because spectral shifts at that angle should be insensitive to convection effects. Based on reference 3, it can be expected that the frequency of peak noise, f_c, at $\theta_I = 90^o$ would be described by equation (1):

$$f_c \propto \frac{V_j}{d} \tag{1}$$

The data in figure 3(a) are for constant d. Therefore, f_c would be proportional to the jet velocities, V_j. The solid curves drawn through the data were generated by translating the same curve shape along the dashed line of $f_c \propto V_j$.

The data vary ±1/2 dB about the curves drawn through the data on figure 3(a). The data are free field above about 400 Hz. The data below that frequency start to show the cancellations and reinforcements typical of ground reflections. Background noise is affecting the low frequency part of the low velocity data; these data were not reported if the background noise was within 2 dB of the measured noise. Internal valve noise has no effect on any data shown on figure 3, or for that matter, any of the data in this report.

In figure 3(b) the SPL spectra are plotted, for $\theta_I = 90^o$ and for four other angles, for the 4-inch nozzle at a high and a low velocity. To avoid clutter the data points are not shown, but the data points are all within 1/2 dB of the curves. Notice that there is a rapid change in the spectral shape (both level and peak noise frequency) near the jet exhaust. Below $\theta_I = 120^o$, the change with θ_I is more gradual. The same results occurred with similar data taken for a 2.06 inch nozzle. These spectra are in good agreement with the data reported in reference 3.

Spatial integration of the axisymmetric SPL spectra at each θ_I results in the sound power level spectra PWL, that are plotted on figure 4(a). The spectra are for the 4-inch diameter nozzle at five velocities. Notice that f_c does not appear to vary with V_j. The curves through the data are again generated by translating the same curve along

the dashed line through the peak noise.

The variation of the PWL spectra with nozzle diameter d, at constant V_j, 600 feet per second, is plotted on figure 4(b). Curves are drawn through the data. The peak noise sound power level scales with d^2 (area) and its center frequency, f_c, are well fit by the dashed line, which is defined by f_c inversely proportional to d. The curves on figure 4(b) collapse together if plotted on a dimensionless power spectral density basis as suggested by Howes (ref. 1).

Discussion of theory. - In a recent paper, Goldstein and Howes (ref. 9), rigorously derived an equation for the total noise intensity in the far field, I. It is based on similar yet less restrictive assumptions than those used by Lighthill (ref. 10). It results in a noise radiation pattern that agrees well with the data. In an abbreviated form, the equation is as follows:

$$I \propto \frac{\rho_o}{c_o^5} \frac{(1 - M_c \cos \theta_J)^{-3}}{r^2} T \tag{2}$$

The convection Mach number is given by $M_c = \beta V_j / c_o$ and θ_J is measured from the jet exhaust. The jet exhaust velocity is given by V_j and β is the ratio of the eddy convection velocity to the jet velocity. The factor $(1 - M_c \cos \theta_J)^{-3}$ represents the effect on the noise radiation pattern of the convection of noise sources by the mean flow. The environmental density and speed of sound are given by ρ_o and c_o, respectively. The term T represents a complex expression that describes the generation of jet noise. It is made up of a self-noise term and a less significant shear noise term. Goldstein points out that T is essentially equivalent to that derived by Lighthill (refs. 10 and 11). Following Lighthill then, this term can be simplified to mean flow terms.

$$T \propto A V_j^8 \tag{3}$$

where A is the exit area of the nozzle. Combining equations (2) and (3) results in

$$I = \frac{K_1}{r^2} \frac{\rho_0}{c_o^5} A V_j^8 \left[1 - \left(\frac{\beta V_j}{c_o} \right) \cos \theta_J \right]^{-3} \tag{4}$$

The principal difference between the result derived by Lighthill (ref. 10) and the equation (4) is the exponent of the factor containing θ_J. Goldstein (eq. (4)) arrived at a -3 exponent while Lighthill obtained an exponent of -5. The axisymmetric intensity described by equation (4) is now integrated over a sphere or radius r to obtain the total power, W.

$$W = K \frac{\rho_o}{c_o^5} A V_j^8 \left[1 - \left(\frac{\beta V_j}{c_o} \right)^2 \right]^{-2} \qquad (5)$$

Goldstein used an experimentally measured value of β (0.62 from ref. 12), which occurs at the center of the mixing region where the most intense turbulence occurs. Along with the -5 exponent, Lighthill used $\beta = 0.5$ (ref. 10), and Lush used $\beta = 0.65$ (based on the work of ref. 13). Equation (4) is a much more sensitive test of the theory than equation (5). Therefore, the next task is to compare the data to the noise radiation pattern predicted by equation (4), where the exponent (-3 or -5) and the value of β (0.62 or 0.5) suggested by the analyses of Goldstein and Lighthill are used.

Noise radiation patterns and comparison to theory. - The SPL spectra for the 4-inch diameter nozzle were integrated over all frequencies to obtain the OASPL noise radiation patterns shown on figure 5. Similar data for a 2.06 inch diameter nozzle, and data taken by Lush (ref. 3), were scaled to the 4-inch nozzle size. They were also corrected for small differences in V_j and the environmental temperature, according to equation (4). These corrected data are also plotted on figure 5. The agreement among the sets of data is excellent. The analytical curves on figure 5 are described by

$$\left(1 - \frac{\beta V_j}{c_o} \cos \theta_J \right)^n$$

These curves are put through the data at $\theta_J = 90^o$ because the data there are not affected by convection. The solid curves are for an exponent of $n = -3$ and $\beta = 0.62$, as suggested by Goldstein (ref. 9); while the dashed curves are for $n = -5$ and $\beta = 0.5$, as suggested by Lighthill (ref. 10). The comparisons at high velocity clearly indicate that the -3 exponent is the better choice. Data from references 1 and 4 also support this conclusion. A better fit of the data was not realized by using a smaller value of β (0.55) with the -3 exponent, as evidenced by the dot-dashed curves on figure 5. The difference between the theory and data for $\theta_I > 160^o$ is probably due to refraction (ref. 14). Refraction was not included in the theories. Reference 15 reported hot jet data for small circular nozzles. The analytical curve, using $n = -3$ and $\beta = 0.62$, still fits the data well except for $\theta_I > 140^o$, where refraction seems to be important.

Total sound power level. - Integration of the SPL spectra spatially and with frequency results in the total sound power level, PWL_T. The PWL_T data for a large range of circular nozzle diameters (1 to 13 in.) are plotted as a function of V_j on figure 6. The subsonic velocities ranged from about 400 to 1100 feet per second. The data were scaled to a nozzle area, A, of 1 ft^2 and an environmental temperature of

77° F according to equation (5). The environmental temperature correction, which affects the ρ_o/c_o^5 term, did not exceed $1\frac{1}{2}$ dB. The plus symbols are data from reference 3. All of the data are in good agreement. The curve drawn through the data is based on equation (5), with β taken as 0.62 because in the previous section it gave a good fit with the noise radiation pattern data. The analytical curve describes the data fairly well. At high velocity the data lie between the analytical curve and a V_j^8 line. The coefficient, K, for the curve (eq. (5)), is 4×10^{-5}, which is in good agreement with the low end of the range of K reported by Lighthill (ref. 11).

Effect of Circular Nozzle Lip Thickness and Length, and Inlet Shape on Noise

In the previous section the noise from a circular nozzle of standard shape (i.e., gradual inlet and short thin lip) was described. In this section, the noise characteristics of circular nozzles with nongradual inlets and long and thick lips will be explored.

Figure 7(a) contains a comparison of the PWL spectra for circular nozzles of different shape at the same peak velocity (same pressure ratio and temperature) and diameter. As for most of the comparisons in this paper, these data were taken during the same day's run so that the repeatability is about 1/2 dB. All of the nozzles shown on figure 7(a) have a fairly high flow coefficient, except the cone-shaped nozzle; and all have a uniform velocity profile at the exit. In spite of the vast differences in inlet and lip shape, all the spectra are within 1 dB of the standard shaped nozzle spectrum. This agreement also occurred at much lower and higher subsonic velocities. The noise radiation patterns for these nozzles also showed that lip thickness and inlet shape had no affect on the subsonic jet noise produced.

The noise from standard shaped nozzles, with a high flow coefficient, is now compared to the noise from nozzles of low flow coefficient (e.g., the cone-shape nozzle and a sharp-edged orifice). These nozzles each have a uniform velocity profile across the exit plane so that the peak (i.e., center line) velocity is the same for the same pressure ratio and temperature. The cone and sharp-edged orifice nozzles have a vena contracta that reduces the effective flow area; therefore, the average velocity is less than the peak velocity. In figure 7(b) the standard nozzle (solid curve) is compared to the cone and sharp-edged orifice, at the same peak velocity (open symbols). These same nozzles are also compared at the same flow or average velocity (closed symbols). Apparently the peak exhaust velocity collapses the noise data, so that it is independent of the nozzle shape, better than the average velocity. The sharp-edged orifice (dashed curve) appears to have an additional high frequency noise source. It may be caused by flow separation as the flow tries to turn around the thick sharp-edged orifice plate.

The effect of nozzle lip length on the noise generated is considered now. The PWL spectra for a standard shaped nozzle, with its short lip, is compared on figure 8 to the spectra for the same nozzle (i.e., same diameter, lip thickness, and inlet shape), but with a 4-foot long lip (30 diameters long). A total pressure probe was used at these nozzle exits so that their centerline (peak) exit velocities could be set equal for this comparison. Figure 8 contains this comparison of the PWL for the short and long lip nozzles at two centerline velocities. Figure 8 also contains a comparison of the velocity profiles. These profiles show that an appreciable turbulent boundary layer built up in the long tube compared to the short lip nozzle. This means that the long lip nozzle had a much less sharp velocity profile (less shear) at the nozzle exit; and therefore a lower turbulence level in the jet mixing region. On the other hand, the turbulence level in the jet "core" leaving the nozzle is much greater for the long lip nozzle. One might also expect some noise to be generated internally by the high velocity flow through the pipe. However, other experiments where the flow passed over large rough surfaces suggest that this would not be an important consideration. For whatever reason, figure 8 clearly shows that the long lip is quieter when compared at the same peak jet velocity and exit diameter. Similar results were obtained with shorter lips (5 and 10 diameters long); however, the noise reduction was less. There is no noise reduction when these data are compared at the same thrust. The same conclusion was reached in an earlier experiment (ref. 16).

At this point the effect of upstream turbulence on jet noise is considered. The long inlet pipe of these jet noise experiments had an inlet pipe area to nozzle area ratio of about 4. Other experimentors, such as Lush (ref. 3), have used higher area ratios. The data taken by Lush for circular nozzles agreed very closely with the data reported herein. But in order to be sure that upstream turbulence would not affect the far field jet noise, a turbulence generator made of a 1 inch wide strip was placed across the 4-inch diameter inlet pipe at a point 5 pipe diameters upstream of a 2.06-inch diameter nozzle. The strip was small enough that it did not by itself generate noise. But it should be expected to generate large eddies which may affect the jet noise generation. However, the far field noise spectra, with and without the turbulence generating strip, were the same (within 1/2 dB) at a high and a low subsonic velocity.

Noise from Plug, Slot, and Other Nozzles

This section deals with some aspects of the noise generated by the subsonic flow issuing from plug, slot, and other nozzles. Slot nozzles of varying aspect ratio are considered first. Then plug nozzles of the same area but different annulus heights are compared. The effect on noise of blunt ended plugs, with their associated base drag, is also considered. Following that, the noise radiation patterns and total power for slot, plug, and circular nozzles are compared. After that, the effect on noise of base drag for a multi-tube nozzle is discussed. Then the noise from orifice plate type nozzles of varying exit plane shapes are

considered, and finally the noise generated by the inner nozzle lip of a coannular nozzle is described.

Slot nozzles. - In figure 9(a) the PWL' spectra are plotted at four velocities, for a slot nozzle with a slot height, h, of 0.5 inch and an aspect ratio (i.e., slot width to height, w/h) of 9. The sound power level spectra, PWL', plotted on figure 9(a), were calculated from the SPL data as if the noise was axisymmetric. They are not quite the true power spectra, PWL. Figure 9(a) contains the PWL' measured in the two perpendicular microphone planes shown. The noise is clearly not axisymmetric. For the cases shown, the true power spectra, PWL, would be nearly half way between the two PWL' that were measured in the $\phi = 0$ and 90^{o} planes.

Figure 9(b) contains a comparison of the PWL' spectra in the $\phi = 90^{o}$ plane that is designed to show the effect of aspect ratio at constant slot height. Three slot nozzles of the same slot height but different aspect ratios (w/h = 3.5, 9, and 69) are compared at a velocity of 953 feet per second. The spectra have been plotted as the difference, PWL'_T - PWL', so that these nozzles of different area can be more easily compared. If the aspect ratio had no affect then these spectral curves would overlap, because the slot height is constant in this comparison. However, it is clear that the aspect ratio does affect the spectra. The frequency of peak noise, f_c, increases as the aspect ratio decreases; but it changes little at large values of w/h. The azimuthal variation of the noise does not affect these conclusions. Data at lower velocities gave the same results. The OASPL directivity and total power for these nozzles are discussed later. The velocity profiles at the exit of these nozzles were measured and found to be uniform along and across the slots.

Plug nozzles. - The free field PWL spectra for three nozzles of the same exit plane area are compared at two velocities on figure 10(a). Two plug nozzles of significantly different annulus heights and plug lengths are compared to a circular nozzle. The plugs are gradually tapered cones so that there is no flow separation. The larger annulus height nozzle shape is the more commonly used geometry. Notice that the PWL spectra for the larger annulus height plug nozzle (h = 0.39 in.) are very nearly the same as the PWL for the 1-5/8 inch diameter circular nozzle. The spectra for the smaller annulus height plug nozzle (h = 0.19 in.) do not coincide with these two; its spectrum has shifted to a higher frequency. The comparison on figure 10(a) shows that the frequency of peak noise, f_c, cannot be simply determined from one dimension (annulus height, h) or the area.

Figure 10(b) shows the effect of blunt-ended plugs (with associated base drag) on noise generation. Three plug nozzles, with an annulus height of 0.39 inch, are compared. The velocity and static pressure pro-

files were measured by the traverse of a pitot static tube near the nozzle exit. The flat-ended plug, which had a steady vacuum or negative pressure (base drag) at the end of the plug, is noisier than the cone-ended plug of figure 10(a), especially at high frequency. The dish ended plug had an unsteady negative pressure and proved to be considerably noisier than the cone ended plug. The flat-ended plug was tested over a range of jet velocities and it was found that the PWL spectra varied with the eighth power of the jet velocity. This implies that the additional noise attributed to base drag was still a quadrupole type of noise source.

Comparison of plug and slot nozzles to the circular nozzle and theory. - Figure 11 contains the variation with nozzle exhaust velocity of the total sound power level, PWL_T and $PWL_T^\dagger$, for the plug and slot nozzles that were discussed on figures 9 and 10(a). These results have been scaled to an exit area, A, of 1 ft^2 and an environmental temperature of 77° F. For comparison, the analytical curve that went through the circular nozzle data of figure 6 is also plotted on figure 11. It is apparent that the data for all nozzles collapse together and the analytical curve describes the results adequately. Because there is an azimuthal variation in the slot nozzle noise, $PWL_T^\dagger$ is plotted for the $\phi = 0°$ and 90° microphone planes. The true total power, PWL_T, is about 1 dB lower than the maximum $PWL_T^\dagger$, which occurs in the $\phi = 90°$ plane. This small correction makes the agreement between the plug, slot, and circular nozzle data even better.

The noise radiation patterns of the slot and plug nozzles are now compared to the analytical curve that fit the circular nozzle data. Goldstein's analysis did not take into account refraction effects, which are important near the jet axis and for the high frequency (relative to f_c) part of the noise spectra. For a given nozzle area this means that slot and plug nozzles of small dimension, h (i.e., relatively high frequency) would probably have more refraction. Refraction normally tends to move the angle of maximum noise back away from the exhaust (see ref. 14).

The noise radiation pattern for the plug nozzles that had sharp cone plugs (annulus heights of 0.39 and 0.19 in.) and the same area, are plotted on figure 12(a). Comparison of the patterns shows that the nozzle with the smaller annulus height (h = 0.19 in.) appears to have a greater refraction effect for $\theta_I > 140°$. The analytical curves defined by $\left(1 - \frac{0.62\ V_j}{c_o} \cos \theta_J\right)^{-3}$ fit the data for larger annulus height nozzle, just as well as they did for the circular nozzle. But refraction apparently affects the pattern for the small annulus height nozzle for $\theta_I > 140°$. The good fit for the larger annulus height is not surprising because the PWL spectra of this plug nozzle and the circular nozzle agree well (see fig. 10(a)). The poor fit of the data at a slightly supersonic ($M_j = 1.02$) velocity of 1030 feet per second is due to weak

shocks which increase the noise near the inlet.

The noise radiation patterns, at $\phi = 90^{o}$, for the 1/2-inch slot height slot nozzles of aspect ratios, w/h, 9 and 69 are compared on figure 12(b) at three velocities. The nozzle data have been scaled to the area and velocities of the larger aspect ratio nozzle (69). The velocity corrections were small (less than $1\frac{1}{2}$ dB). A small correction (less than $1\frac{1}{2}$ dB) has been consistently applied to the OASPL to account for the fact that, in some case when h is small, the 20 kHz data limit cuts off the SPL roll-off too quickly. The patterns for the two slot nozzles agree quite well except for $\theta_I > 140^{o}$. One representative noise radiation pattern in the $\phi = 0^{o}$ plane for the 69 to 1 aspect ratio slot nozzle at V_j = 761 feet per second, has also been plotted on figure 12(b) for comparison. The refraction effect is less pronounced in the sideline ($\phi = 0^{o}$) plane. The analytical curves that fit the circular and plug nozzle data also fit the slot nozzle patterns except for $\theta_I > 140^{o}$.

Multi-tube nozzle base drag. - The additional noise caused by plug base drag (a negative pressure) was demonstrated on figure 10(b). A multi-tube nozzle also has potential base drag caused by poor ventilation between the tubes, which could lead to additional noise. In addition, multiple jets (e.g., suppressor nozzle) can conceivably be quieter. Poor ventilation may adversely affect this favorable result. The noise spectra, PWL, from a 19-tube nozzle (fig. 2(f)), with long tubes and good ventilation, is plotted for two peak exhaust velocities on figure 13. The space between the tubes was then filled with clay, flush to the tube ends, and noise data were again taken at the same velocities. In this case, the ventilation of the inner tubes is poor as evidenced by the negative pressure measured between the tube exits. It was shown before (fig. 7(a)) that lip thickness had no affect on noise. And the clay fill-in does not affect the velocity profiles at the nozzle exits. Therefore, this comparison (i.e., clay to no clay) will give some idea of the effect of ventilation on noise generation. According to figure 13 the arrangement with poor ventilation is noisier, especially at high frequency.

Subsonic screech. - Figure 14 demonstrates that a screech (discreet frequency) can occur for a nozzle at subsonic velocities. The nozzles in this case are various shaped orifice holes of the same total area that were cut into large flat plates (8 in. square) (see fig. 2(g)). At a higher velocity (965 ft/sec) only the vertical slot screeched. Many of these same nozzle exit plane shapes were tested with relatively long tapered inlets. These nozzles did not screech. It appears that screech can occur subsonically when the noise is generated close to a large nozzle surface. The point of this section is that this type of nozzle shape should be avoided in jet noise experiments.

Coannular nozzle lip noise. - The last item to discuss is the additional noise that can be generated by a coannular nozzle lip. In the case of the coannular nozzle, shown by figure 2(h), high velocity streams flow

past either side of the inner nozzle lip causing a local region of stagnation and high shear downstream of that lip. The nozzle in figure 2(h) has a 0.1 inch thick lip, a 2.06 inch diameter core nozzle, and a secondary to core nozzle area ratio of 5.4. The PWL spectra for this nozzle are plotted on figure 15 for a core velocity of 800 feet per second and a number of secondary to core velocity ratios ranging from 0 to 1. The additional noise caused by the inner nozzle lip occurs at high frequency and is quite pronounced. The "lip noise" measured is a narrow band noise but it is not a discrete tone. It occurred at all subsonic core velocities and for other nozzle sizes. It also occurred for a coannular nozzle with a centerbody and when the core nozzle extended well beyond the secondary nozzle. Figure 15 shows that as the velocity ratio decreases from 1, the frequency of this noise decreases a little. Finally, this noise disappears for velocity ratios below about 0.5. From the data on figure 15 and other data, it appears that the Strouhal number for "lip noise," based on the lip thickness and core velocity, would be about 0.2. However, this is a tentative conclusion because the only lip thickness tested at this time has been 0.1 inch. If this conclusion is correct, then low noise engines should not be built with any thick lips whenever high velocity streams are on both sides of the lip. The investigators in reference 17 also observed this additional noise in their coannular nozzle experiments. The noise radiation pattern for this additional noise alone (i.e., "lip noise" spectra removed from total spectra measured) peaked near $\theta_I = 100^o$ to 120^o.

CONCLUDING REMARKS

For a circular nozzle at subsonic velocities the nozzle inlet shape and lip thickness had no effect on the noise level or spectra. The data from these nozzles were compared at the same nozzle exit diameter and peak exhaust velocity. A sharp edged orifice was one exception to this statement; it had some additional high frequency noise. The effect of a very long nozzle lip was to reduce the noise when compared at the same peak velocity. Blunt ended center bodies, where there is significant base drag due to inadequate ventilation, generate significant additional noise. When the two streams of a coannular nozzle mix, there is a stagantion zone at the lip of the inner nozzle that generates additional very high frequency noise. When the outer nozzle velocity is less than about half the inner nozzle velocity, this noise disappears.

It was found that the total noise power generation was essentially the same for circular, slot, and plug nozzles of good aerodynamic design. The noise radiation patterns for subsonic flow were essentially the same for these nozzle shapes, wherever refraction was not important. The noise radiation pattern data was well fit by $(1 - M_c \cos \theta_J)^{-3}$ which is the theoretical result derived by Goldstein.

SYMBOLS

A	nozzle area at exhaust exit plane, ft^2
C_1, C_2	cancellation frequencies of ground reflections, Hz
C_v	flow coefficient
c_o	speed of sound in environment, ft/sec
d	nozzle diameter, ft
d_p	plug diameter at throat, ft
f	third octave band center frequency, Hz
f_c	center frequency, frequency of peak noise, Hz
h	slot height, plug annulus height, ft
I	total intensity, W/ft^2
K_1, K	coefficients defined by eqs. (4) and (5)
L	plug length from nozzle exit plane, ft
M_c	convection Mach number
n	exponent
OASPL	overall sound pressure level, dB
PWL	sound power level, dB
PWL_T	total sound power level, dB
PWL', PWL_T'	measure of PWL and PWL_T when noise not axisymmetric; calculated as if noise were axisymmetric, dB
R_1, R_2	reinforcement frequencies of ground reflections, Hz
r	distance from noise source to observer, ft
SPL	sound pressure level, dB
T_o	environmental temperature, ^oF
t	nozzle lip thickness, ft
V_j	peak nozzle exhaust velocity, ft/sec

W	total power, W
w	slot nozzle width, ft
β	convection velocity/exhaust velocity
θ_I	angle from nozzle inlet, deg
θ_J	angle from nozzle jet exhaust, $\theta_J = 180 - \theta_I$, deg
ρ_o	density of environment, lbm/ft^3
T	defined by eqs. (2) and (3)
ϕ	microphone plane; see fig. 9(a)

REFERENCES

1. Howes, W. L., "Similarity of Far Noise Fields of Jets," TR R-52, 1959, NASA, Cleveland, Ohio.

2. Maestrello, L. and McDaid, E., "Acoustic Characteristics of High-Subsonic Jet," AIAA Journal, Vol. 9, No. 6, June 1971, pp. 1058-1066.

3. Lush, P. A., "Measurements of Subsonic Jet Noise and Comparison with Theory," Journal of Fluid Mechanics, Vol. 46, Pt. 3, Apr. 13, 1971. pp. 477-500.

4. Krishnappa, G. and Csanady, G. T., "An Experimental Investigation of the Composition of Jet Noise," Journal of Fluid Mechanics, Vol. 37, Pt. 1, June 5, 1969, pp. 149-159.

5. Lilley, G. M., "Comments on Some Unsolved Problems in Jet-Noise Research," Basic Aerodynamic Noise Research, SP-207, 1969, NASA, Washington, D.C., pp. 511-513.

6. Luidens, R., et al., "Engine Noise Technology," STOL Technology, SP-320, NASA, Washington, D.C.

7. Dorsch, R. G., Kreim, W. J., and Olsen, W. A., "Externally-Blown-Flap Noise," Paper 72-129, Jan. 1972, AIAA, New York, N.Y.

8. Olsen, W., Miles, J., and Dorsch, R., "Noise Generated by Impingement of a Jet Upon a Large Flat Board," TN D-7075, 1972, NASA, Cleveland, Ohio.

9. Goldstein, M. and Howes, W., "New Aspects of Subsonic Aerodynamic Noise Theory," TN D-7158, 1973, NASA, Cleveland, Ohio.

10. Lighthill, M. J., "Sound Generated Aerodynamically," Proceedings of the Royal Society of London, Ser. A, Vol. 267, No. 1329, May 8, 1962, pp. 147-182.

11. Lighthill, M. J., "On Sound Generated Aerodynamically. I. General Theory," Proceedings of the Royal Society of London, Ser. A, Vol. 211. No. 1107, Mar. 20, 1952, pp. 564-587.

    Lighthill, M. J., "On Sound Generated Aerodynamically. II. Turbulence as a Source of Sound," Proceedings of the Royal Society of London, Ser. A, Vol. 222, No. 1148, Feb. 23, 1954, pp. 1-32.

12. Wills, J. A. B., "On Convection Velocities in Turbulent Shear Flows," Journal of Fluid Mechanics, Vol. 20, Pt. 3, Nov. 1964, pp. 417-432.

13. Davies, P. O. A. L., Fisher, M. J., and Varratt, M. J., "The Characteristics of the Turbulence in the Mixing Region of a Round Jet," Journal of Fluid Mechanics, Vol. 15, Pt. 3, Mar. 1963, pp. 337-367.

14. Ribner, H. S., "Quadrupole Correlation Governing the Pattern of Jet Noise," Journal of Fluid Mechanics, Vol. 38, Pt. 1, Aug. 14, 1969, pp. 1-24.

15. Hoch, R. G. and Cocking, B. J., "Studies of the Influence of Density on Jet Noise," presented at the First International Symposium on Air-Breathing Engines, Marseille, France, June 1972.

16. Powell, A., "The Influence of the Exit Velocity Profile on the Noise of a Jet, " ARC-16156, Sept. 1953, Aeronautical Research Council, Great Britain.

17. Bielak, G., "Coaxial Flow Jet Noise," DGE-10041-1, 1971, Boeing/Aeritalia, Seattle, Wash.

TABLE I. - NOZZLE DIMENSIONS

Noise data plotted on figure	Nozzle shape referenced to figure 2	Nozzle exit plane shape	Nozzle diameter d, in.	Total nozzle exit area, A, $in.^2$	Lip thickness t, in.	Other dimensions and comments	
3,4,5,6	2(a-1,2)	Circular	4.	12.6	0.125	Standard shape	
4(b),6	↓	↓	3.06	7.35	↓	↓	
4,6			2.06	3.3			
4(b),6			1.625	2.1			
4(b),6			1.06	.875			
6			13.	132.			
7	2(a-1)	Circular	1.63	2.1	0.06	Standard shape; thin lip, gradual inlet	
	2(a-2)	↓	↓	↓	.125	Standard shape; thicker lip, gradual inlet	
	2(a-3)				1.5	Very thick lip; gradual inlet	
	2(a-4)				-----	Rounded inlet orifice	
	2(a-5)				0.125	Cone inlet, sharp lip	
	2(a-6)				-----	Sharp-edged orifice	
8	2(b-1)	↓	↓	↓	0.125	Short lip, same as (a-2)	
	2(b-2)				.125	Long lip, 4 ft long	
	2(c)	Slot	N/A			Slot height, h, in.	Slot width/height, w/h
9(b),11	↓	↓	↓	0.84	0.125	0.5	3.5
9(a),11, 12(b)				2.1	.125	.5	9
9(b),11, 12(b)				18.8	.1	.524	69
11				3.5	.125	.9	4.5
10(a),11	2(d-1)	Circular	1.63	2.1	.125		

TABLE I. - Concluded. NOZZLE DIMENSIONS

Noise data plotted on figure	Nozzle shape referenced to figure 2	Nozzle exit plane shape	Nozzle diameter d, in.	Total nozzle exit area, A, $in.^2$	Lip thickness t, in.	Other dimensions and comments		
						Plug diam, d_p, in.	Annulus height, h, in.	Plug length, L, in.
10(a),11	2(d-2)	Cone plug	2.06	2.1	1.25	1.28	0.39	3.7
11	2(d-2)		4.	6.45		2.8	.6	8.
10(a),11	2(d-3)		4.05	2.1		3.67	.19	13.
10(h)	2(e-1,2,3)	Cone, flat and dished ended plugs	2.06	2.1	0.125	1.28	0.39	See fig. 2(e)
13	2(f)	19 tubes	0.55	4.57	0.06	19 tubes, 3" long		
14	2(g)	Varied	Varied	2.1	----	See fig. 2(g)		
15	2(h)	Coannular	2.08,5.4	3.2,17.6	0.1	See fig. 2(h)		

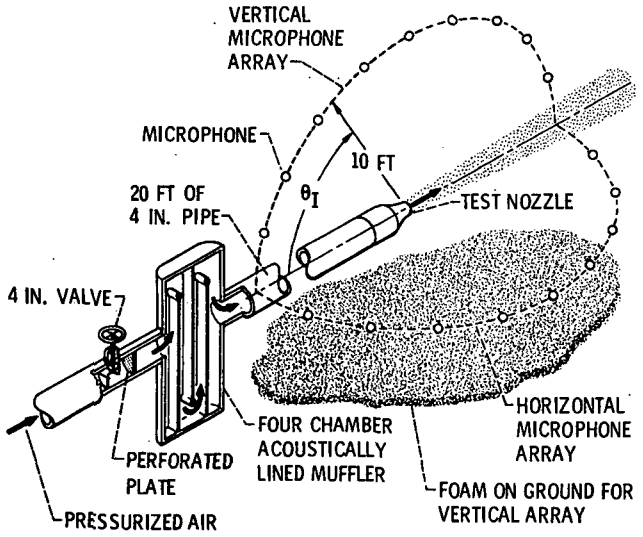

Figure 1. - Flow system for small nozzle tests with both semi-circular microphone arrays shown.

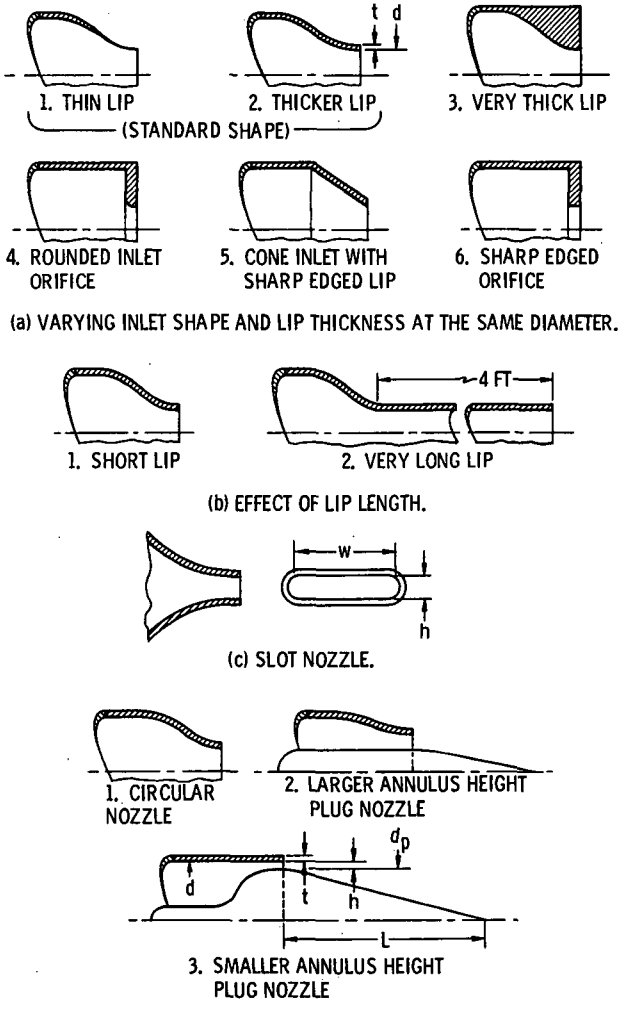

Figure 2. - Sketches of nozzles tested. Dimensions tabulated in table I.

(e) EFFECT OF PLUG END.

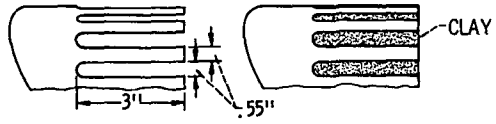

1. WELL VENTILATED
2. SPACE BETWEEN TUBES FILLED WITH CLAY UP TO TUBE ENDS

(f) EFFECT OF VENTILATION FOR MULTI-TUBE NOZZLE (19 TUBES).

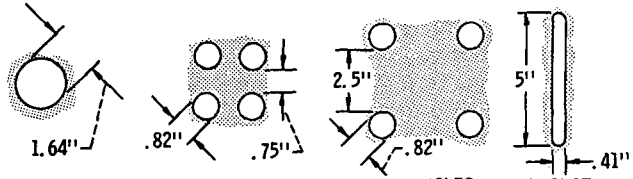

1. ONE HOLE
2. FOUR HOLES CLOSE TOGETHER
3. FOUR HOLES FAR APART
4. SLOT

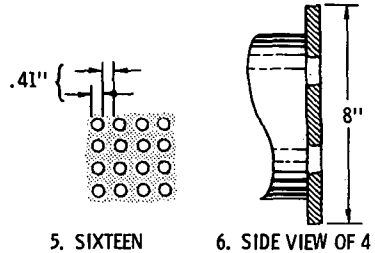

5. SIXTEEN HOLES
6. SIDE VIEW OF 4 HOLE NOZZLE.

(g) ORIFICE PLATE NOZZLES OF VARYING SHAPED HOLES BUT SAME TOTAL AREA,

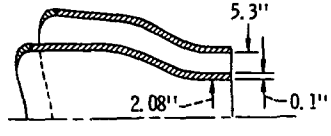

(h) COANNULAR NOZZLE.

Figure 2. - Concluded.

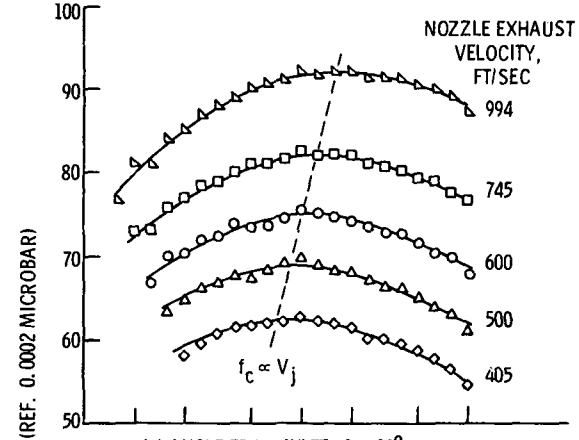

(a) ANGLE FROM INLET, θ_I, 90^0.

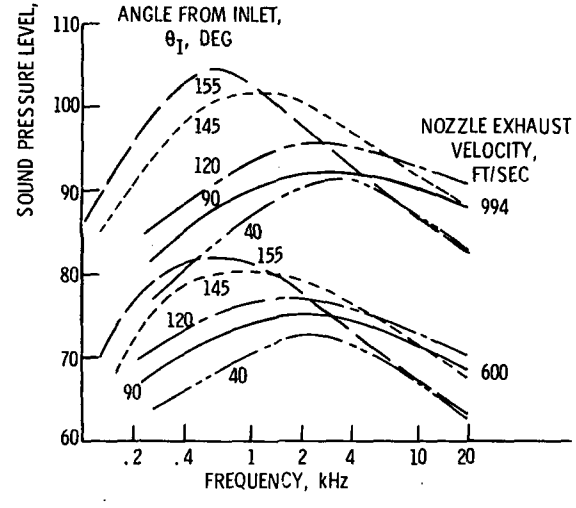

(b) AT SEVERAL ANGLES, θ_I, DEG

Figure 3. - Sound pressure level spectra for standard shaped circular nozzle at a number of velocities. Nozzle diameter 4-inches; environmental temperature, 77^0 F; free field lossless data taken on a 15 ft radius.

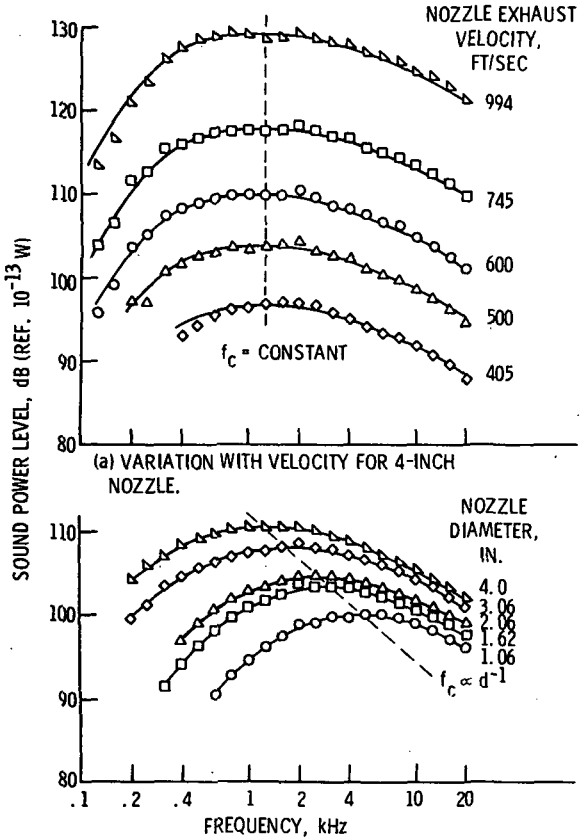

(a) VARIATION WITH VELOCITY FOR 4-INCH NOZZLE.

(b) VARIATION WITH DIAMETER AT CONSTANT VELOCITY, 600 FT/SEC.

Figure 4. - Sound power level spectra for standard shaped circular nozzles. Environmental temperature, 77° F; free field lossless data.

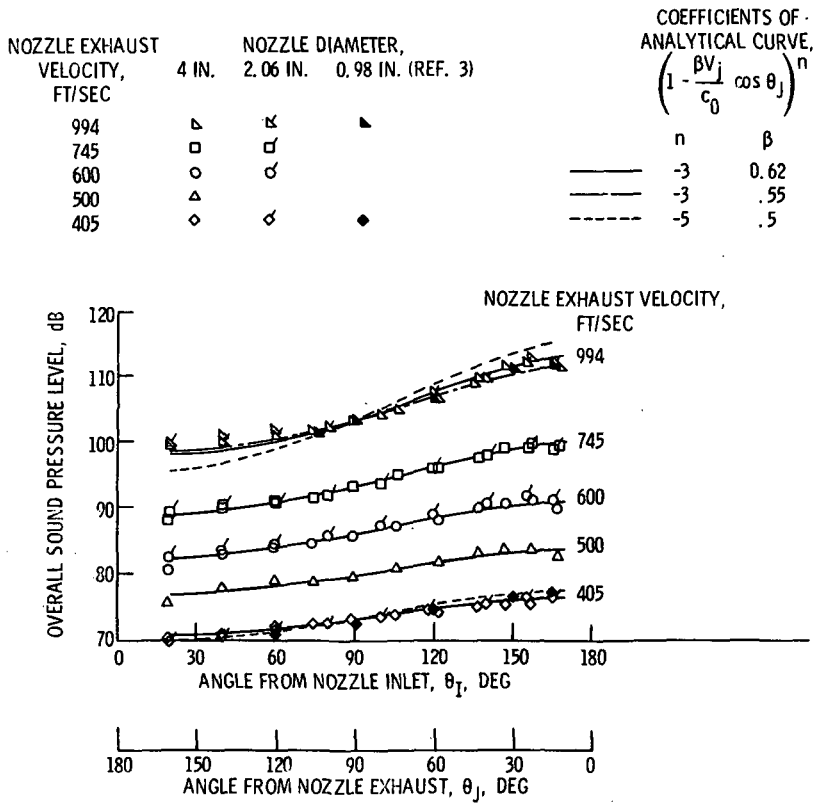

Figure 5. - Noise radiation pattern at 15 feet for circular nozzles. All data scaled to same nozzle diameter, 4 inches, and ambient temperature, 77° F. Free field lossless data.

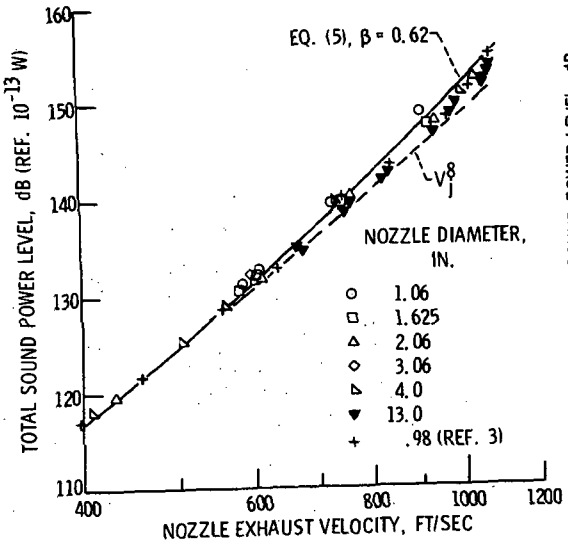

Figure 6. - Variation of total sound power level with jet velocity for circular nozzles. All data scaled to an area of 1 ft^2 and an ambient temperature of 77° F. Free field lossless data.

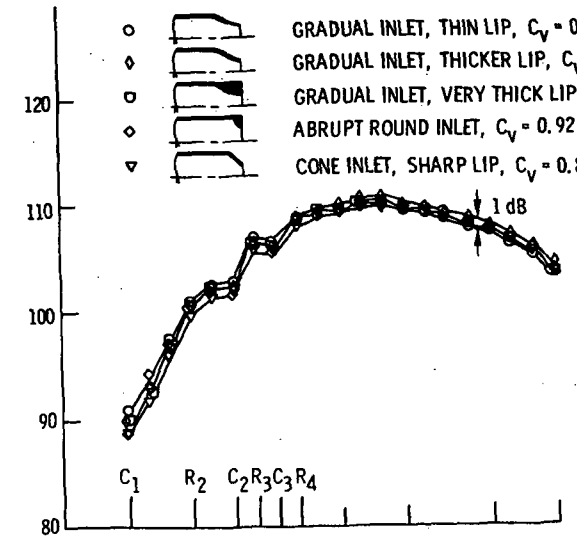

(a) NOZZLES COMPARED AT CONSTANT PEAK VELOCITY, 785, FT/SEC.

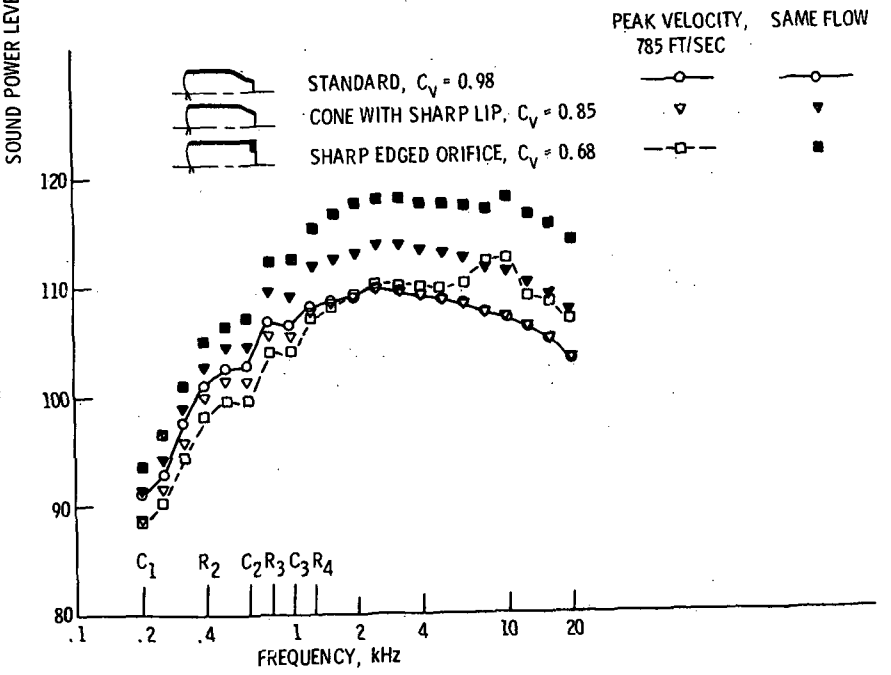

(b) NOZZLES WITH LOW FLOW COEFFICIENTS ARE COMPARED AT SAME PEAK VELOCITY, AND ALSO AT SAME AVERAGE VELOCITY, OR FLOW.

Figure 7. - Effect of nozzle inlet and lip shape. Nozzle diameter, 1-5/8 inches; Ground reflection cancellations and reinforcement frequencies denoted below by C_i and R_i, respectively.

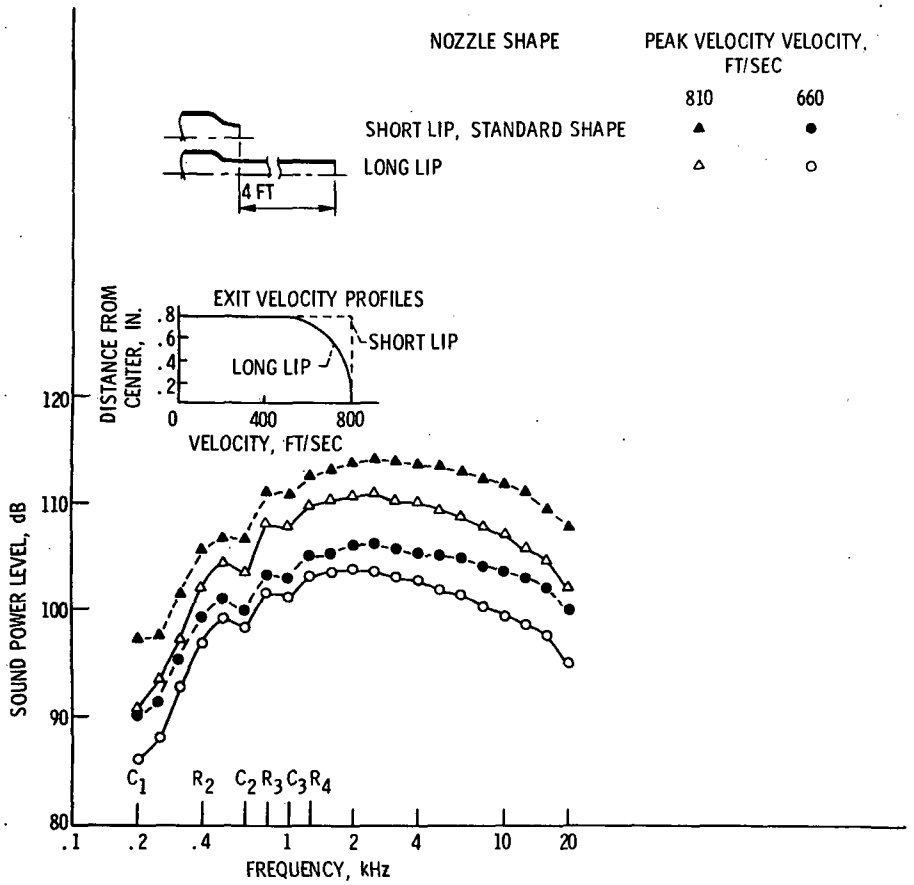

Figure 8. - Effect of nozzle lip length at same peak exhaust velocity. Nozzle diameter, 1-5/8 inches; lip thickness, 1/8 inch; Ground reflection cancellations and reinforcements, frequencies denoted by C_i and R_i, respectively.

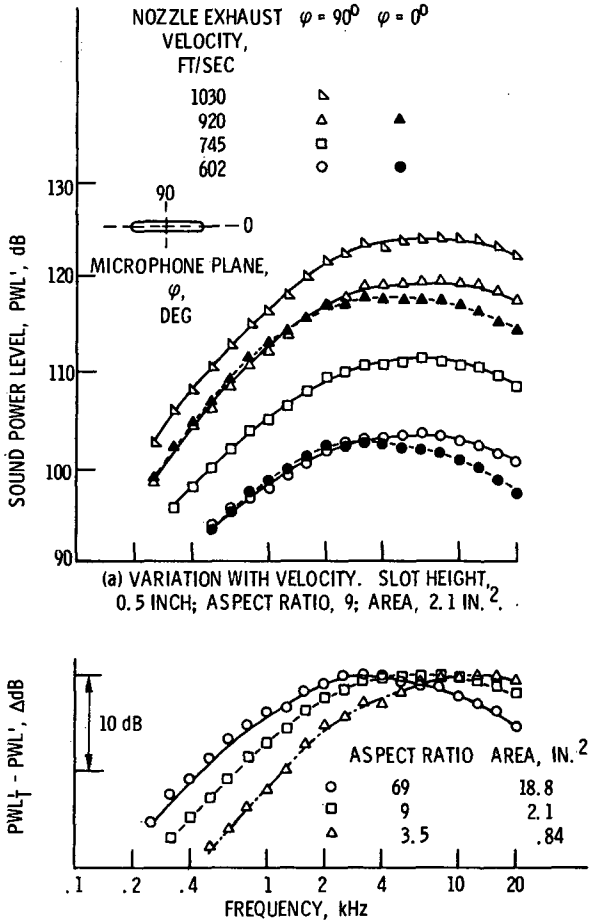

(b) EFFECT OF ASPECT RATIO ON SLOT NOZZLE SPECTRA AT SAME SLOT HEIGHT, 0.5 IN., AND VELOCITY, 950 FT/SEC; $\varphi = 90^0$.

Figure 9. - Sound power level spectra for slot nozzles, evaluated at φ. Environmental temperature, 77^0 F; free field lossless data.

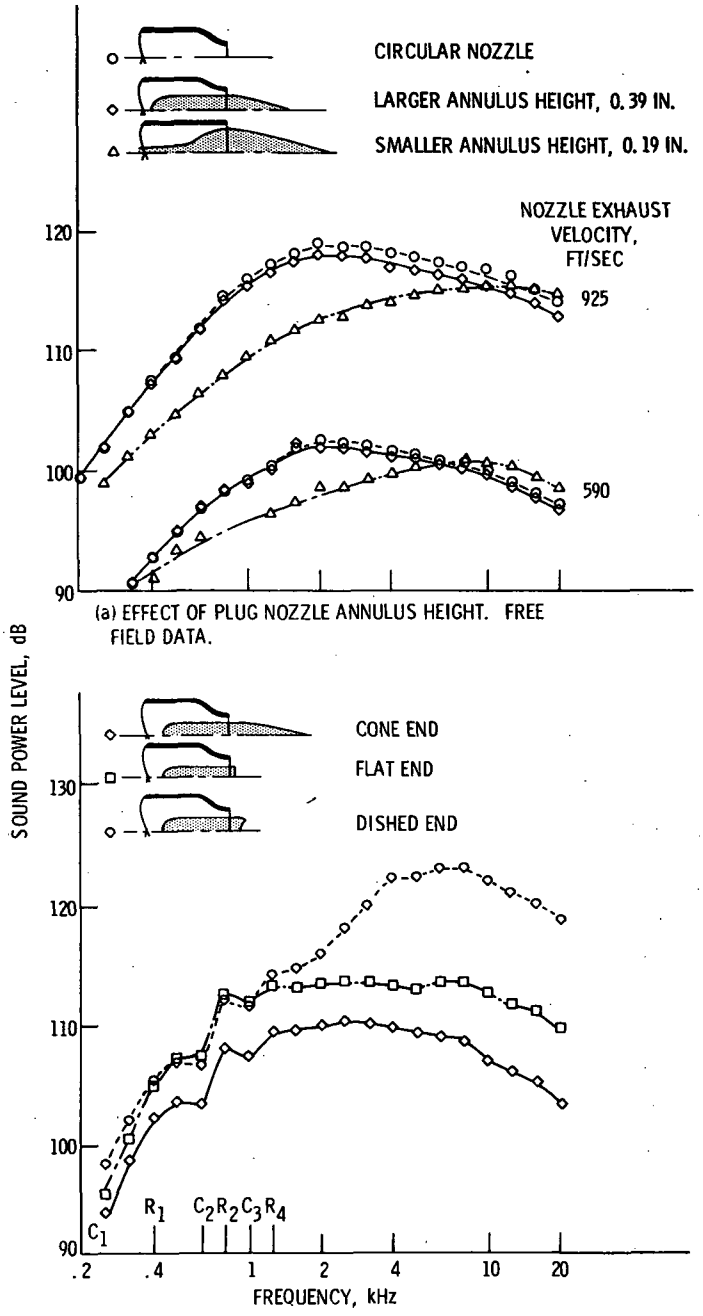

(a) EFFECT OF PLUG NOZZLE ANNULUS HEIGHT. FREE FIELD DATA.

(b) EFFECT OF PLUG END SHAPE; VELOCITY, 785 FT/SEC. ANNULUS HEIGHT, 0.39 IN. GROUND REFLECTIONS PRESENT.

Figure 10. - Sound power level spectra for plug nozzles. Nozzle area, 2.1 in.^{2}; environmental temperature, 77^0 F; lossless data.

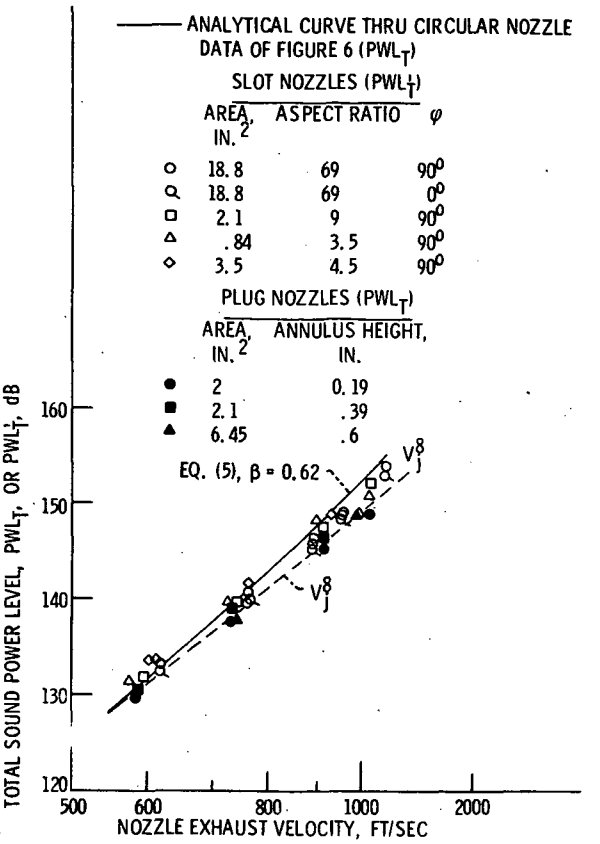

Figure 11. - Variation of total sound power level with nozzle exhaust velocity for slot, plug and circular nozzles of standard shape. All data scaled to an area of 1 ft^2, and ambient temperature of 77^0 F. Free field lossless data.

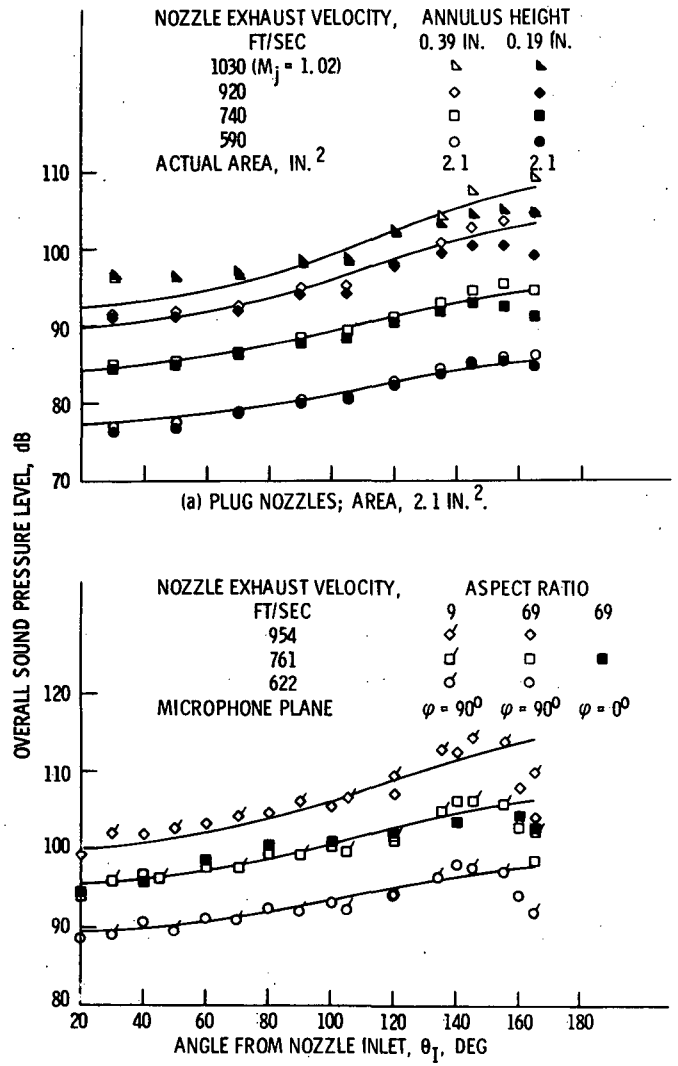

(a) PLUG NOZZLES; AREA, 2.1 IN.^{2}.

(b) SLOT NOZZLES SCALED TO SAME AREA, 18.8 IN.^{2}, SLOT HEIGHT, 0.5 IN.

Figure 12. - Noise radiation pattern at 10 feet for plug and slot nozzles at several velocities. All data scaled to same ambient temperature, 77^0 F. Free field lossless data. Analytical curves drawn thru open symbol data at θ_I = 90^0 using β = 0.62 and n = -3.

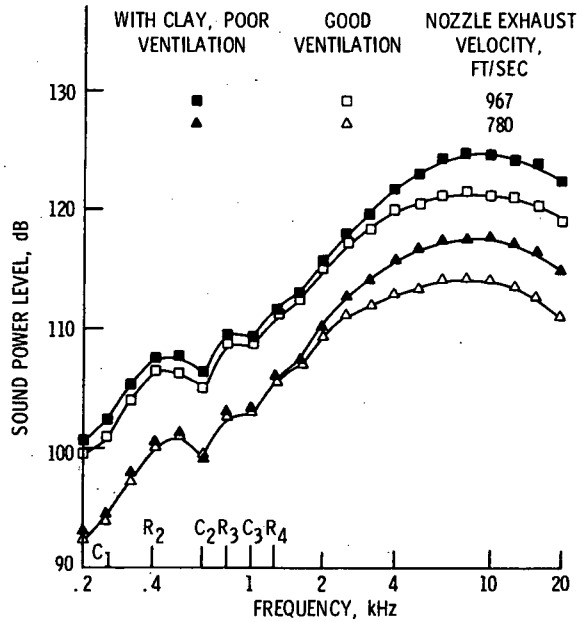

Figure 13. - Effect of ventilation on multi-tube nozzle noise. Nineteen tube nozzle; tube diameter, 0.56 inch; tube length, 3 inch.

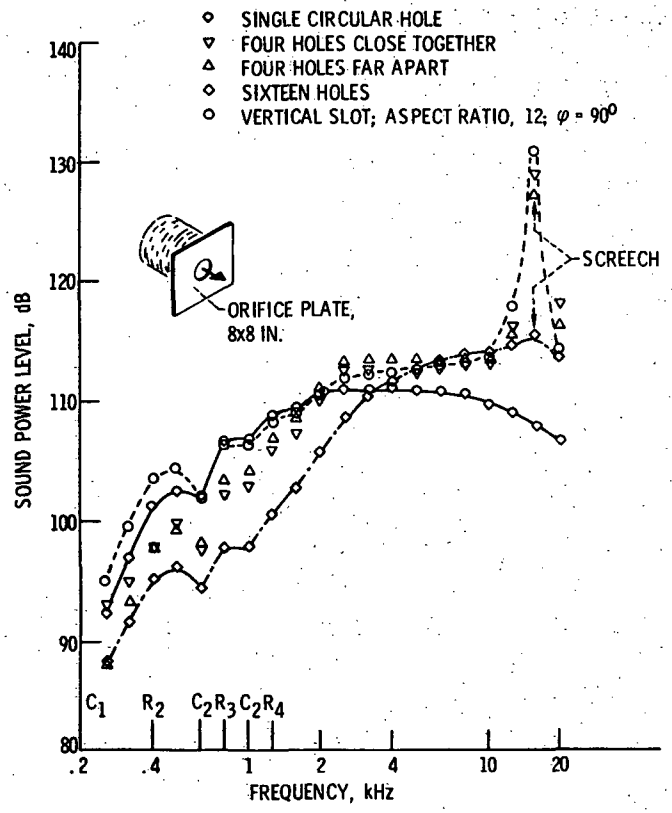

Figure 14. - Some examples of nozzle screech. Nozzle exhaust velocity, 770 ft/sec; nozzle area, 2.1 $in.^2$.

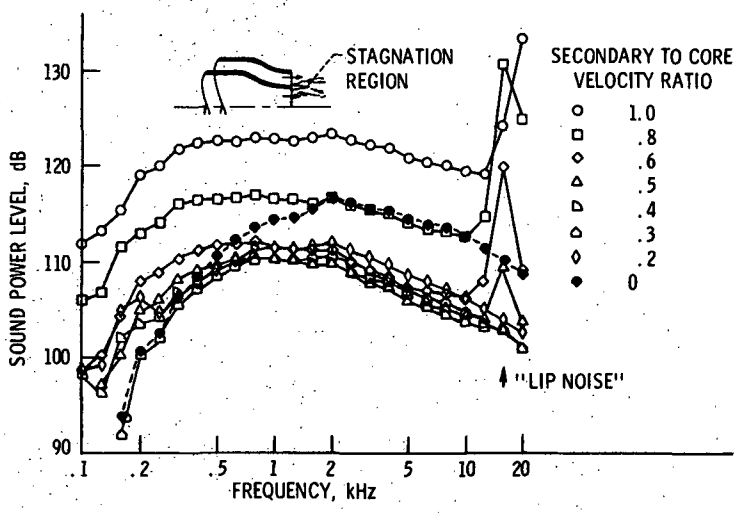

Figure 15. - Coannular nozzle "lip noise." Core velocity, 800 ft/sec; core diameter, 2.08 inch; area ratio, 5.4; lip thickness, 0.1 inch. Free field lossless data.